SCIENTIFIC REPORTS

OPEN

SUBJECT AREAS:

SUPERCONDUCTING PROPERTIES AND MATERIALS

APPLIED PHYSICS

CHARACTERIZATION AND ANALYTICAL TECHNIQUES

Received
16 June 2014

Accepted
31 July 2014

Published
22 August 2014

Correspondence and requests for materials should be addressed to C.B. (cbarone@unisa.it)

Probing transport mechanisms of $BaFe_2As_2$ superconducting films and grain boundary junctions by noise spectroscopy

C. Barone[1,2], F. Romeo[1,2], S. Pagano[1,2], M. Adamo[2], C. Nappi[3], E. Sarnelli[3], F. Kurth[4] & K. Iida[4]

[1]Dipartimento di Fisica ''E.R. Caianiello'', Università di Salerno, I-84084 Fisciano, Salerno, Italy, [2]CNR-SPIN Salerno, Università di Salerno, I-84084 Fisciano, Salerno, Italy, [3]CNR-SPIN Napoli, Via Campi Flegrei 34, I-80078 Pozzuoli, Napoli, Italy, [4]Leibniz-Institut für Festkörper- und Werkstoffforschung (IFW) Dresden, PO Box 270116, 01171 Dresden, Germany.

An important step forward for the understanding of high-temperature superconductivity has been the discovery of iron-based superconductors. Among these compounds, iron pnictides could be used for high-field magnet applications, resulting more advantageous over conventional superconductors, due to a high upper critical field as well as its low anisotropy at low temperatures. However, the principal obstacle in fabricating high quality superconducting wires and tapes is given by grain boundaries. In order to study these effects, the dc transport and voltage-noise properties of Co-doped $BaFe_2As_2$ superconducting films with artificial grain boundary junctions have been investigated. A specific procedure allows the separation of the film noise from that of the junction. While the former shows a standard 1/f behaviour, the latter is characterized by an unconventional temperature-dependent multi-Lorentzian voltage-spectral density. Moreover, below the film superconducting critical temperature, a peculiar noise spectrum is found for the grain boundary junction. Possible theoretical interpretation of these phenomena is proposed.

The presence of high angle grain boundaries (GBs) has severely limited the use of high-T_c cuprate superconductors in developing practical applications, such as superconducting wires and tapes[1]. Iron-based superconductors, for their metallic nature in the normal state, small anisotropy in superconducting properties, and a highly symmetric order parameter (i.e., $s_{\pm}$-pairing)[2], seem to be more favourable than cuprates with respect to the supercurrent conduction across the high angle GBs and, as a consequence, more attractive for applications[3–6]. In particular, Co-doped $BaFe_2As_2$ compound appears to have great potential for devices realization, due to the easy film growth by pulsed laser deposition (PLD) and chemical stability at ambient atmosphere[7,8]. The study of electrical conduction in grain boundary junctions (GBJs) based on this class of materials is, therefore, important for a better understanding of the current transport mechanisms and for improvement of their performances[9,10]. Among different spectroscopic techniques, electric noise analysis has already been used for the sensitive investigation of charge carriers kinetic processes in several systems, such as conducting oxides[11–13], electron-doped cuprate superconductors[14], and iron chalcogenides[15,16]. After the seminal work by Koch *et al.*[17], measurements of the low-frequency electric noise in various superconducting GBJs have been reported in literature[18,19]. However, the fluctuations spectroscopy in junctions based on iron pnictides has never been investigated and is open to both experimental and theoretical activity.

In view of all these issues, a detailed characterization and interpretation of the noise-spectral density in $Ba(Fe_{0.92}Co_{0.08})_2As_2$ films and GBJs is here presented. The samples, having thickness of 100 nm and deposited by PLD on roof-type bicrystal substrates, have been subsequently patterned by ion beam etching to form several geometrical configurations with characteristic size from 2 to 100 μm. The results of the experimental investigations performed on a representative 2.6 μm wide strip are shown in the following, together with a discussion and analysis of possible theoretical explanations. A brief description of the experimental procedures and methods is also given.

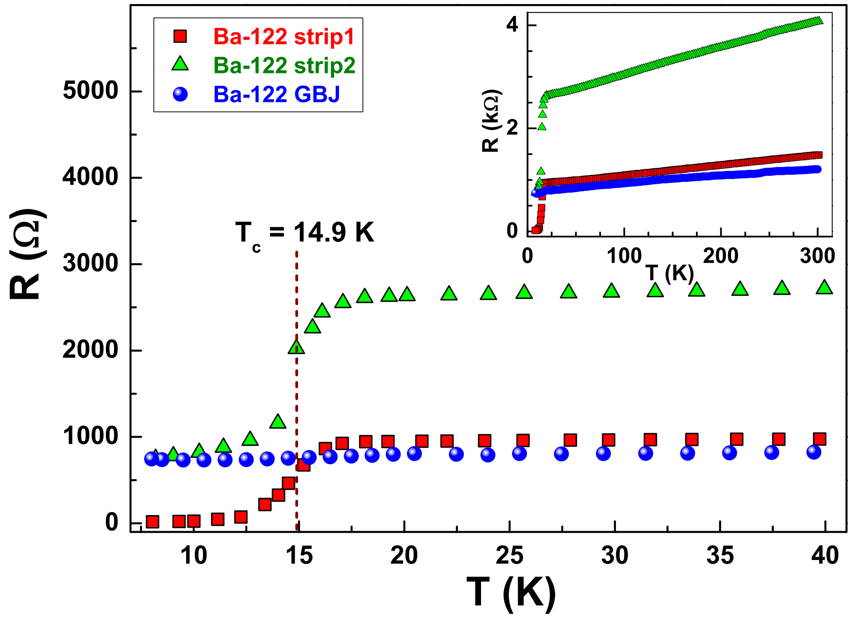

Figure 1 | **Resistance versus temperature data.** Red squares refer to the strip1; green triangles refer to the strip2; blue circles refer to the intrinsic GBJ, whose resistance values are computed from equation (1). The superconducting transition temperature of the film, defined at 50% of normal state resistance, is also reported. In the inset, the full investigated temperature range is shown.

Results

Electric transport measurements. The temperature dependence of the resistance is shown in Fig. 1 for the strip1 without the GBJ (R^{strip1}) and for the strip2 containing the GBJ (R^{strip2}), as red squares and green triangles, respectively. The superconducting transition of the film occurs at a critical temperature $T_c = (14.9 \pm 0.1)$ K, defined at 50% of normal state resistance. This value is somewhat lower than that of the bulk compounds, probably due to film processing and ageing. A full superconductivity is observed for the strip1, while a residual resistance is found in presence of GBJ, related to a relatively thick barrier produced by the high angle roof-type GB bicrystal substrate. The intrinsic GBJ resistance can be computed from the experimental data, by removing the strip contribution, as

$$R^{GBJ} = R^{strip2} - R^{strip1} r_g, \quad (1)$$

where $r_g \simeq 1.93$ is a resistance rescaling factor from strip1 to strip2 which takes into account their specific geometrical configuration. The temperature dependence of R^{GBJ}, obtained from equation (1), is shown in Fig. 1 as blue circles. It is evident that no visible variation is present crossing T_c, while a linear, metal-like, behaviour is observed in the whole temperature range (see the inset of Fig. 1 for details). The Ohmic nature of the samples is also confirmed by linear current-voltage characteristics, found at all investigated temperatures. It is worth noting that the presence of a 20 nm Fe buffer layer could introduce a parallel conduction path. However, this seems not to be the case here, as the measured resistivity of the samples is close to that obtained in absence of Fe buffer layer[20]. This is probably due to the interdiffusion of Co, Ba, and As in the Fe layer during the fabrication process[21], resulting in a strong increase of the buffer layer resistivity.

Voltage-noise characterizations. A detailed electric noise analysis has been performed on the strip1 and the strip2 in absence and in presence of the GBJ, respectively. The experimental voltage-spectral densities, measured between 10 and 300 K, are shown in Fig. 2 at three representative temperatures (i.e., above T_c, below T_c, and just T_c) by employing the same bias current of 1 mA. They are all characterized by the same frequency dependence, which can be well reproduced by the following expression[22]

$$S_V(f, I, T) = \frac{K(I, T)}{f^{\gamma(T)}} + C(T). \quad (2)$$

In equation (2), $K(I, T)$ is the low-frequency noise amplitude; $\gamma(T)$ is the frequency exponent, usually ranging from 1 (pure 1/f-type noise) to 2 (pure Lorentzian-type noise); and $C(T)$ is the frequency-independent noise component, due to the sample Johnson noise $4k_BTR(T)$ and to the readout electronic chain noise (for the employed setup it is 1.4×10^{-17} V^2/Hz). By assuming a homogeneous distribution of fluctuators in the whole sample and using the volume noise dependence from the well-known semi-empirical Hooge formulation[22], it is possible to compute the intrinsic grain boundary voltage-spectral density (S_V^{GBJ}) by subtracting the strip contribution. Hence

$$S_V^{GBJ} = S_V^{strip2} - S_V^{strip1} s_g, \quad (3)$$

where $s_g \simeq 0.18$ is the voltage-noise geometrical factor evaluated according to the Hooge expression. This procedure allows to show that, for the strip2 the low-frequency noise is essentially produced by fluctuations occurring in the GBJ region, the strip noise being more than one order of magnitude lower. As a consequence, information on the conduction mechanisms and on the dynamic behaviours of the charge carriers in the GBJ can be obtained with a systematic study of the noise amplitude K as a function of the bias current. However, as is always the case with noise measurements, a technique to rule out extrinsic contact noise contributions has to be performed[23]. After such procedure, the analyzed results show that K has a net quadratic bias current dependence for all the strips and investigated temperatures (see in Supplementary Fig. 1). Therefore, the source of electric noise can be ascribed to pure resistance fluctuations[22]. This type of fluctuations is usually modeled by using a simple parabolic functional form as $K(I, T) = a_2(T) I^2$, where a_2 is a temperature-dependent parameter. The observed quadratic dependence down to very low current values (50 μA), together with linear I–V characteristics, rule out any possible Joule heating effect.

The physical mechanism producing the measured resistance fluctuations can be identified by studying the temperature evolution of the frequency exponent γ of equation (2). This dependence appears

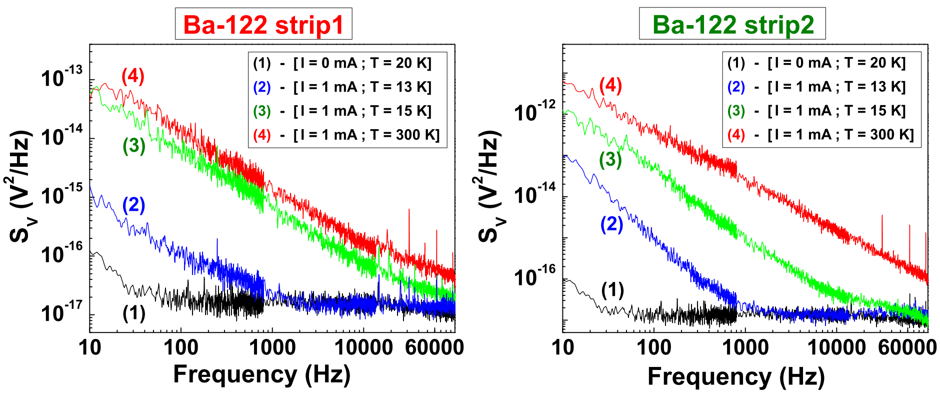

Figure 2 | **Voltage-noise spectra.** The spectral densities, at three reference temperatures and at a fixed bias current, are shown for the strip1 (left panel) and for the strip2 (right panel). The traces (1) black are the zero-bias background noise.

as a very striking feature in Fig. 3, in the case of the GBJ noise-spectral density. More in detail, for strip1, without GBJ, γ shows very small variations around the average value 1.00 ± 0.01 in the whole investigated temperature range (red open squares in Fig. 3). This means that Co-doped Ba-122 film is characterized by pure 1/f noise spectra, as observed in several common metals and conventional superconductors[22]. By using the strip1 as a reference system, it is possible to compute the frequency exponent of the GBJ voltage-noise-spectral density. In this case, Fig. 3 (blue full circles) shows that γ decreases linearly in temperature going from 1.5 at T_c, to 1.2 at 300 K. Moreover, a step-increase up to 2 is found below T_c. This indicates that, although resistance fluctuations are the source of GB noise, the mechanism of such fluctuations is unconventional. These experimental findings can be interpreted by assuming that only a limited number of current coupled fluctuators are present in the small GBJ volume. This number is progressively reduced by decreasing the temperature, compatibly with a thermally activated process. Such mechanism can be accounted for, under the assumption that the relaxation time τ of a generic fluctuator is given by $\tau = \tau_0 \exp[\delta E/(k_B T)]$, where δE represents the activation energy of the thermal process. In large sample volumes, δE can be considered as a uniformly distributed stochastic variable within the interval $[E_{min}, E_{max}]$, and the distribution of relaxation times describing the fluctuators population is given by $\mathcal{D}(\tau) = \frac{k_B T}{E_{max} - E_{min}} \tau^{-1}$. This leads to the usual 1/f noise. On the other hand, for very small volumes it is more reasonable to assume that δE is a Gaussian random variable. Then, $\mathcal{D}(\tau)$ is a log-normal distribution, well approximated by $\mathcal{D}(\tau) \sim \tau^{-\alpha}$ with $0 < \alpha < 2$ [24]. Within the multi-Lorentzian model of low-frequency noise[25,26], the spectral density of the whole system is defined as $S_V \sim \int_0^{\infty} \frac{4\tau \mathcal{D}(\tau)}{1 + (\omega\tau)^2} d\tau$. By simple substitution, one obtains $S_V^{\alpha}(\omega) \sim 2\pi \csc\left(\frac{\pi\alpha}{2}\right) \omega^{\alpha-2}$. In this framework, the frequency exponent is $\gamma = 2 - \alpha$ and can take values between 1 and 2, depending on the number of active fluctuators. Its experimental temperature dependence, above the critical temperature, can be reproduced in terms of the following functional form

$$\gamma(T) = \gamma_0 - BT. \tag{4}$$

The best fitting expression of equation (4) is obtained with $\gamma_0 = (1.50 \pm 0.01)$ and $B = (1.010 \pm 0.015) \times 10^{-3}\ K^{-1}$, and is shown in Fig. 3 as a solid line.

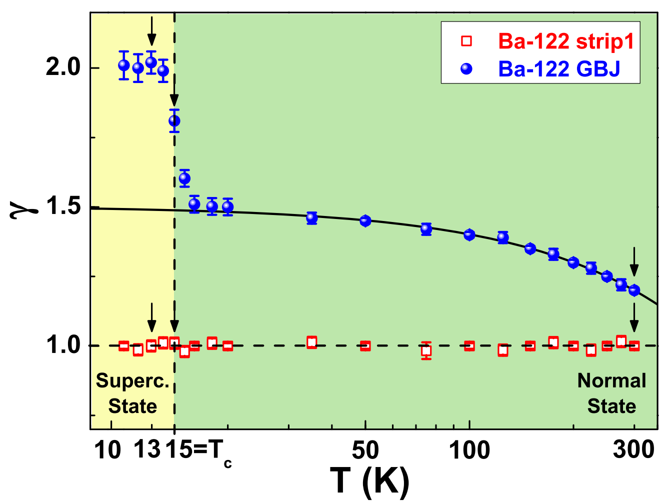

Figure 3 | **Temperature dependence of the frequency exponent** γ. Red open squares refer to the strip1; blue full circles refer to the intrinsic GBJ. The value for strip2 is the same as for the GBJ, being the latter the dominant noise source. The horizontal dashed line corresponds to the mean value $\gamma = (1.00 \pm 0.01)$. The solid line is the best fitting curve by using equation (4). The arrows correspond to the temperatures shown in Fig. 2. Note the logarithmic temperature scale.

This allows to determine the temperature dependence of the distribution function $\mathcal{D}(\tau)$, thus providing information for the development of a microscopic model of thermally activated fluctuations in the system. The sharp transition of the frequency exponent at T_c, however, implies a strong reduction in the number of fluctuators correlated with the superconducting transition. In order to clarify the physical mechanisms involved in this feature, quite evident in Fig. 3, further indications can be acquired by evaluating the sample voltage-noise level NL. For Ohmic systems, as the case here reported, NL is defined as[22]

$$NL = \frac{Var[V]}{V^2} = \int_{f_{min}}^{f_{max}} df \frac{S_V(f,I,T)}{[R(T)I]^2}, \tag{5}$$

where the frequency interval $[f_{min}, f_{max}]$ is the experimental bandwidth. By using equation (2) and substituting the specific expression of $K(I, T)$ for resistance fluctuation processes, it is straightforward to compute from equation (5)

$$NL \approx \frac{a_2(T)}{R(T)^2} \times \begin{cases} \ln\left(\frac{f_{max}}{f_{min}}\right), & \gamma = 1, \\ \frac{f_{max}^{1-\gamma} - f_{min}^{1-\gamma}}{1-\gamma}, & \gamma \neq 1. \end{cases} \tag{6}$$

In equation (6) the Johnson noise component has been neglected, because is much smaller than the a_2 contribution. From equation (6) it is possible to estimate the intrinsic noise level, whose temperature dependence is shown in Fig. 4 for the strip1 (red open squares) and the strip2 (green open triangles), respectively. It is evident that *NL* of strip1 is characterized by a constant amplitude in the normal state. A noise peak is observed near the transition temperature, a well-known feature related to a superconducting percolation transition and reported for other high-T_c compounds[27–29]. Below T_c, the *NL* is strongly suppressed by the superconducting state. The strip2, with the GBJ, shows higher values of *NL* and the same noise peak near T_c, also related to the film transition. An analysis in terms of a percolative model accounts for the noise peak near T_c in both strips, and allows to express the resistance dependence of *NL* above T_c as $NL \propto R(T)^{-l_{rs}}$[30]. The exponent l_{rs} is a critical index related to the dimensionality of the percolating network in the transition region. A value $l_{rs} = (2.74 \pm 0.04)$ is found for strip1 and strip2, indicating a three-dimensional (3D) percolating network for the film[30]. By using the appropriate geometrical rescaling, similar to equation (3), from equation (6) it is possible to compute the intrinsic GBJ noise level, whose temperature dependence is shown in Fig. 4 as blue full circles. The main features of the GBJ *NL* are an almost constant value above T_c, a small peak at T_c, and a smaller constant value below T_c. The relatively high *NL* value is the direct consequence of a smaller resistance compared to that of the strips. The less pronounced noise peak at T_c could be a residual of the rescaling procedure caused by a slightly different T_c for the two strips. Below T_c, the almost constant noise level is associated to the abrupt transition of the frequency exponent from 1.5 to 2 (see Fig. 3).

Discussion

The observed experimental behaviour could be explained in different ways essentially related to specific properties of the junction. In this respect, it is important to underline that in the GB region the current path could be considered as divided into several microbridges characterized by different Sharvin conductance[31]. Although, below T_c, a clear dc Josephson current is not seen, it is not possible to exclude that a small fraction of the microbridges constitutes Josephson weak-links with very small critical current I_c. Its fluctuation (rms $I_c \approx e\Delta/\hbar$, see ref. 32) can be of the same order of its average value, producing fast switching of the link between a normal and a superconducting state. According to this scenario, a small number (fluctuating in time) of very fragile Josephson weak-links could be randomly created in the GBJ. Such links support higher current density, compared to normal links, and thus can be much more effective in perturbing the state of the fluctuators active in their neighborhood. The reduced number of effective fluctuators activated by such mechanism is consistent with the observation of a Lorentzian spectrum, which is measured in the GB junction.

An alternative explanation involves the two-gap nature of the iron-based superconductors. In the framework of the $s_{\pm}$-pairing model, the left L (right R) side of the GB junction is characterized by two gaps, namely $\Delta_i^{(L/R)} \exp\left(i\phi_i^{L/R}\right)$ with $i = \{1, 2\}$ the band index, having phase difference $\phi_1^{(L/R)} - \phi_2^{(L/R)} = \pi$. Consequently, the Josephson current I_J presents two contributions: one is related to the coupling between order parameters having the same band index ($\Delta_i^{(L)}$ coupled to $\Delta_i^{(R)}$) and determining a *direct* component of the Josephson current $I_c^{(d)}\sin(\theta)$, with θ the phase difference between the left and right side of the junction; the second one is induced by the coupling of order parameters having different band index and it leads to a *crossed* contribution $I_c^{(c)}\sin(\theta+\pi)$. If the direct and crossed Josephson channels contribute to the observed current with probability p and $q = 1 - p$, respectively, the expectation value of the Josephson current is $E[I_J] = \left(pI_c^{(d)} - qI_c^{(c)}\right)\sin(\theta)$, while its variance is $Var[I_J] = pq\left(I_c^{(d)} + I_c^{(c)}\right)^2 \sin^2(\theta)$. The above argument implies that, even when the effective critical current $\bar{I}_c = \left(pI_c^{(d)} - qI_c^{(c)}\right)$ is small, its variance (or rms) is not negligible. Furthermore the quantity $Var[I_J]/E[I_J]^2$ should be temperature independent, if the two order parameters appear at the same critical temperature and follow the Bardeen, Cooper, Schrieffer (BCS) temperature dependence. The GBJ tunneling probability can be locally modulated by an impurity vibration with a low-frequency switching time, responsible for a change in the overlap of the wavefunctions of different bands at the interface. Under these assumptions, a dc Ohmic behaviour is expected, while a random telegraph noise induced by the switching of direct/crossed Josephson channel affects the fluctuations, giving rise to the observed Lorentzian spectrum. The above scenario, even though not unambiguously verified in the present work, deserves further investigations since it could be an important fingerprint of the fluctuation properties of Josephson devices based on multiband superconductors.

In conclusion, the low-frequency noise of Co-doped Ba-122 films and GBJs show distinctive behaviours. By suitable geometrical rescaling, the resistive and noise components of the film and of the GBJ can be separately analyzed. The film has a regular 1/f noise, a quadratic current dependence, and shows a 3D percolating network behaviour near T_c. The bicrystal junction noise also shows a quadratic current dependence but with an anomalous frequency dependence, and has nonzero amplitude with a Lorentzian spectrum below T_c. The pres-

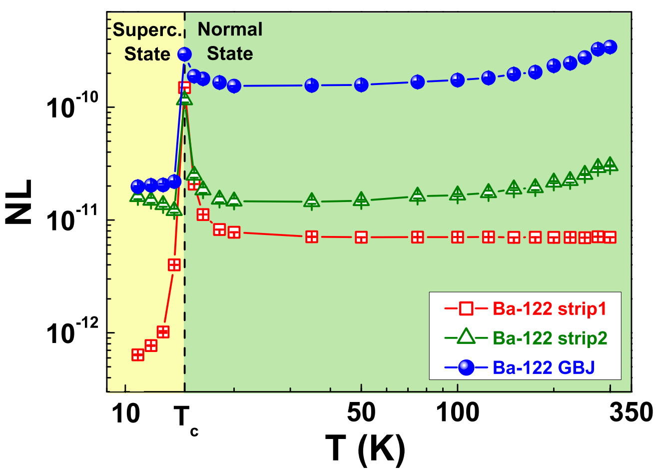

Figure 4 | Noise level experimental behaviour. The temperature dependence of the noise level *NL*, defined in equation (6), is shown for the strip1 (red open squares), for the strip2 (green open triangles), and for the intrinsic GBJ (blue full circles). The lines are guides to the eyes.

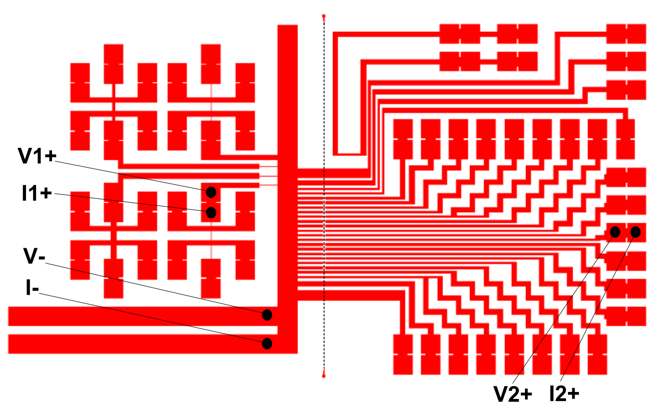

Figure 5 | Layout of the strips patterned on the bicrystal substrate. The vertical black dashed line represents the bicrystal boundary. The black dots indicate the contact pads for strip1 and strip2.

ence of a small number of fluctuating Josephson weak-links seems to be a crucial ingredient to explain the noise in the superconducting state of the GBJ.

Methods

Epitaxial $Ba(Fe_{0.92}Co_{0.08})_2As_2$ films (100 nm thick) were deposited by pulsed laser deposition on $Fe/MgAl_2O_4$-buffered roof-type bicrystal $SrTiO_3$ substrates, having a misorientation angle of 45°. The details of the fabrication process are reported in ref. 33. Several strips, having width from 2 to 100 μm, have been patterned by a standard photoresist process followed by ion beam etching. Some strips were designed to include an artificial grain boundary junction induced by the bicrystal substrate. All the junctions with different widths were analyzed, showing very similar results. As specified above, here are reported the data relative to a representative 2.6 μm wide strip, whose geometrical configuration of the contact pads is shown in Fig. 5. In particular, strip1 is without GBJ (left side), while strip2 contains the GBJ, which is represented with a dashed line in Fig. 5 (right side).

All the measurements were performed by using a closed-cycle refrigerator, operating in the 8- to 325-K range. The temperature stabilization, better than 0.1 K, has been realized through a computer-controlled feedback loop. The achieved stability was sufficient to record stable spectral data at all temperatures. Near T_c, the intrinsic resistance fluctuations produce a substantial increase of noise, as described above. The core of the experimental setup is based on a very low-noise electronics, in order to reduce external spurious contributions to the measured spectral signal.

1. Larbalestier, D., Gurevich, A., Feldmann, D. M. & Polyanskii, A. High-T_c superconducting materials for electric power applications. *Nature* **414**, 368–377 (2001).
2. Mazin, I. I., Singh, D. J., Johannes, M. D. & Du, M. H. Unconventional Superconductivity with a Sign Reversal in the Order Parameter of $LaFeAsO_{1-x}F_x$. *Phys. Rev. Lett.* **101**, 057003 (2008).
3. Gao, Z. *et al.* High critical current density and low anisotropy in textured $Sr_{1-x}K_xFe_2As_2$ tapes for high field applications. *Sci. Rep.* **2**, 998 (2012).
4. Iida, K. *et al.* Oxypnictide SmFeAs(O,F) superconductor: a candidate for high-field magnet applications. *Sci. Rep.* **3**, 2139 (2013).
5. Zhang, X. *et al.* Realization of practical level current densities in $Sr_{0.6}K_{0.4}Fe_2As_2$ tape conductors for high-field applications. *Appl. Phys. Lett.* **104**, 202601 (2014).
6. Zhang, W.-H. *et al.* Direct observation of high-temperature superconductivity in one-unit-cell FeSe films. *Chin. Phys. Lett.* **31**, 017401 (2014).
7. Katase, T. *et al.* Atomically-flat, chemically-stable, superconducting epitaxial thin film of iron-based superconductor, cobalt-doped $BaFe_2As_2$. *Solid State Commun.* **149**, 2121–2124 (2009).
8. Iida, K. *et al.* Strong T_c dependence for strained epitaxial $Ba(Fe_{1-x}Co_x)_2As_2$ thin films. *Appl. Phys. Lett.* **95**, 192501 (2009).
9. Lee, S. *et al.* Weak-link behavior of grain boundaries in superconducting $Ba(Fe_{1-x}Co_x)_2As_2$ bicrystals. *Appl. Phys. Lett.* **95**, 212505 (2009).
10. Katase, T. *et al.* Josephson junction in cobalt-doped $BaFe_2As_2$ epitaxial thin films on $(La,Sr)(Al,Ta)O_3$ bicrystal substrates. *Appl. Phys. Lett.* **96**, 142507 (2010).
11. Savo, B., Barone, C., Galdi, A. & Di Trolio, A. dc transport properties and resistance fluctuation processes in Sr_2FeMoO_6 polycrystalline thin films. *Phys. Rev. B* **73**, 094447 (2006).
12. Wu, X. D. *et al.* Nonequilibrium 1/f noise in low-doped manganite single crystals. *Appl. Phys. Lett.* **90**, 242110 (2007).
13. Méchin, L. *et al.* 1/f noise in patterned $La_{2/3}Sr_{1/3}MnO_3$ thin films in the 300–400 K range. *J. Appl. Phys.* **103**, 083709 (2008).
14. Barone, C., Guarino, A., Nigro, A., Romano, A. & Pagano, S. Weak localization and 1/f noise in $Nd_{1.83}Ce_{0.17}CuO_{4+\delta}$ thin films. *Phys. Rev. B* **80**, 224405 (2009).
15. Barone, C. *et al.* Thermal and voltage activated excess 1/f noise in $FeTe_{0.5}Se_{0.5}$ epitaxial thin films. *Phys. Rev. B* **83**, 134523 (2011).
16. Barone, C. *et al.* Electric field activated nonlinear 1/f fluctuations in Fe(Te, Se) superconductors. *Supercond. Sci. Technol.* **26**, 075006 (2013).
17. Koch, R. H., Van Harlingen, D. J. & Clarke, J. Quantum-Noise Theory for the Resistively Shunted Josephson Junction. *Phys. Rev. Lett.* **45**, 2132–2135 (1980).
18. Mück, M., Korn, M., Mugford, C. G. A., Kycia, J. B. & Clarke, J. Measurements of 1/f noise in Josephson junctions at zero voltage: Implications for decoherence in superconducting quantum bits. *Appl. Phys. Lett.* **86**, 012510 (2005).
19. Eroms, J. *et al.* Low-frequency noise in Josephson junctions for superconducting qubits. *Appl. Phys. Lett.* **89**, 122516 (2006).
20. Lee, S. *et al.* Template engineering of Co-doped $BaFe_2As_2$ single-crystal thin films. *Nature Mater.* **9**, 397–402 (2010).
21. Kurth, F. *et al.* Electronic phase diagram of disordered Co doped $BaFe_2As_{2-\delta}$. *Supercond. Sci. Technol.* **26**, 025014 (2013).
22. Kogan, S. *Electronic Noise and Fluctuations in Solids* (Cambridge University Press, Cambridge, 1996).
23. Barone, C. *et al.* Experimental technique for reducing contact and background noise in voltage spectral density measurements. *Rev. Sci. Instrum.* **78**, 093905 (2007).
24. Bak, P., Tang, C. & Wiesenfeld, K. Self-organized criticality: An explanation of the 1/f noise. *Phys. Rev. Lett.* **59**, 381–384 (1987).
25. Ishioka, S., Gingl, Z., Choi, D. & Fuchikami, N. Amplitude truncation of Gaussian $1/f^{\alpha}$ noises. *Phys. Lett. A* **269**, 7–12 (2000).
26. Watanabe, S. Multi-Lorentzian Model and 1/f noise spectra. *J. Korean Phys. Soc.* **46**, 646–650 (2005).
27. Testa, J. A. *et al.* 1/f-noise-power measurements of copper oxide superconductors in the normal and superconducting states. *Phys. Rev. B* **38**, 2922–2925 (1988).
28. Maeda, A., Nakayama, Y., Takebayashi, S. & Uchinokura, K. 1/f conduction noise in the high-temperature superconductor Bi-Sr-Ca-Cu-O system. *Physica C* **160**, 443–448 (1989).
29. Bobyl, A. V. *et al.* Resistance flicker noise and current percolation in c-oriented $YBa_2Cu_3O_{7-x}$ films in the vicinity of T_c. *Physica C* **247**, 7–33 (1995).
30. Kiss, L. B. & Svedlindh, P. New noise exponents in random conductor-superconductor and conductor-insulator mixtures. *Phys. Rev. Lett.* **71**, 2817–2820 (1993).
31. Miklich, A. H., Clarke, J., Colclough, M. S. & Char, K. Flicker (1/f) noise in biepitaxial grain boundary junctions of $YBa_2Cu_3O_{7-x}$. *Appl. Phys. Lett.* **60**, 1899–1901 (1992).
32. Beenakker, C. W. J. Universal limit of critical-current fluctuations in mesoscopic Josephson junctions. *Phys. Rev. Lett.* **67**, 3836–3839 (1991).
33. Iida, K. *et al.* $BaFe_2As_2$/Fe bilayers with [001].-tilt grain boundary on MgO and $SrTiO_3$ bicrystal substrates. *Phys. Procedia* **45**, 189–192 (2013).

Acknowledgments

The authors would like to thank S. Abate of CNR-SPIN Salerno for his technical support. The research leading to these results has received funding from European Union's Seventh Framework Programme (FP7/2007–2013) under grant agreement number 283141 (IRON-SEA).

Author contributions

C.B., F.R. and S.P. wrote the main manuscript text. E.S. and K.I. wrote the Methods. The electric transport and voltage-noise measurements were performed by C.B. and S.P., while F.R., C.N. and E.S. contributed to the theoretical interpretation of the experimental findings. The investigated films were prepared and structurally characterized by F.K. and K.I., and M.A. was principally involved in the sample patterning. All authors discussed the results and implications, and commented on the manuscript by reviewing it accurately.

Additional information

Supplementary information accompanies this paper at http://www.nature.com/scientificreports

Competing financial interests: The authors declare no competing financial interests.

How to cite this article: Barone, C. *et al.* Probing transport mechanisms of $BaFe_2As_2$ superconducting films and grain boundary junctions by noise spectroscopy. *Sci. Rep.* **4**, 6163; DOI:10.1038/srep06163 (2014).